BMC Medicine

RESEARCH

Open Access

Deep learning-aided optical biopsy achieves whole-chain diagnosis of Correa cascade of gastric cancer: a prospective study

Guanqun Liu[1,2,3†], Guangchao Li[1,2,3†], Zhen Li[1,2,3*], Xuejun Shao[4], Rui Ji[1,2,3], Tian Ma[1,2,3], Yan Zhang[1,2,3], Jingran Su[1,2,3], Qingqing Qi[1,2,3], Jing Guo[1,2,3], Yishan He[1,2,3], Xiaoxiao Yang[1,2,3], Yanqing Li[1,2,3] and Xiuli Zuo[1,2,3*]

Abstract

Background Biopsies are essential in differentiating benign from malignant lesions in routine gastroscopy. Nevertheless, redundant biopsies increase patients' expenses and pathologists' workload. Probe-based confocal laser endomicroscopy (pCLE) enables real-time in vivo histological evaluation for gastric neoplasms and precancerous conditions. However, endoscopists vary widely in skill, and the use of pCLE requires histopathology expertise, which limits its application in nonacademic settings. This study aimed to develop a pCLE computer-aided diagnosis system (CCADS) for real-time whole-chain diagnosis of Correa cascade of gastric cancer and evaluate it in a real clinical setting.

Methods Gastric pCLE images and videos from 5771 examinations were retrospectively collected. CCADS was constructed using deep learning networks. It was developed using 47,462 pCLE images and 461 video segments and evaluated via multistep validation. A total of 11,439 images and 667 videos were identified for offline validation. Consecutive patients from October 2019 to September 2021 were enrolled in a prospective diagnostic study for real-time validation, which included 951 patients in the statistics. Blinded expert endoscopists and CCADS independently performed real-time pCLE diagnosis of gastric mucosal lesions in routine examinations, with double-read histopathology as the gold standard. The real-time diagnostic performance of CCADS was evaluated and compared with that of experts.

Results CCADS achieved high diagnostic performance in image test, video test, and a prospective diagnostic study with a large sample size. Overall, 1254 lesions from 951 patients were included in the prospective test. The real-time diagnostic accuracies of CCADS for inflammation, atrophy, gastric intestinal metaplasia (GIM), low-grade intraepithelial neoplasia (LGIN), and high-grade intraepithelial neoplasia and gastric cancer (HGIN/CA) were 91.71%–97.13%. CCADS achieved high sensitivity (98.44%) and specificity (97.06%) for HGIN/CA. Compared with experts, CCADS achieved similar accuracies in diagnosing atrophy, GIM, and LGIN and similar sensitivities in all five categories. Further, CCADS showed a significantly higher sensitivity (96.70% vs. 89.01%, $p = 0.044$) for gastric neoplasms (LGIN + HGIN/CA) and reduced the misdiagnosis of neoplasms.

†Guanqun Liu and Guangchao Li contributed equally to the study.

*Correspondence:
Zhen Li
qilulizhen@sdu.edu.cn
Xiuli Zuo
zuoxiuli@sdu.edu.cn
Full list of author information is available at the end of the article

© The Author(s) 2025. **Open Access** This article is licensed under a Creative Commons Attribution-NonCommercial-NoDerivatives 4.0 International License, which permits any non-commercial use, sharing, distribution and reproduction in any medium or format, as long as you give appropriate credit to the original author(s) and the source, provide a link to the Creative Commons licence, and indicate if you modified the licensed material. You do not have permission under this licence to share adapted material derived from this article or parts of it. The images or other third party material in this article are included in the article's Creative Commons licence, unless indicated otherwise in a credit line to the material. If material is not included in the article's Creative Commons licence and your intended use is not permitted by statutory regulation or exceeds the permitted use, you will need to obtain permission directly from the copyright holder. To view a copy of this licence, visit http://creativecommons.org/licenses/by-nc-nd/4.0/.

Conclusions CCADS achieved expert-level whole-chain diagnosis of Correa cascade. It could assist endoscopists in improved surveillance of gastric neoplasms and precancerous conditions, promote the application of pCLE, and reduce biopsies.

Trial registration ClinicalTrials.gov Identifier: NCT03784209.

Keywords Optical biopsy, Artificial intelligence, Gastric neoplasms, Gastric precancerous conditions

Background

Gastric cancer ranks fifth in incidence and third in cancer-related mortality worldwide [1]. Although early recognition is possible, most gastric cancers are diagnosed at advanced stages, resulting in high patient mortality and a heavy burden on healthcare systems [1]. In the Correa cascade, intestinal-type gastric adenocarcinoma is preceded by the inflammation–atrophy–metaplasia–dysplasia–carcinoma sequence [2]. Early identification, appropriate surveillance, and management of precancerous conditions (atrophic gastritis, gastric intestinal metaplasia (GIM)), precancerous lesions (low-grade intraepithelial neoplasia (LGIN), high-grade intraepithelial neoplasia [HGIN]), and early gastric cancer are essential to improve patient prognoses [3].

Endoscopy is the most common and important method for detecting gastric lesions. Biopsies are essential in routine gastroscopy because gastropathy cannot be reliably distinguished from gastritis using white-light endoscopy (WLE) [4]. Although endoscopic techniques such as magnifying endoscopy (ME), chromoendoscopy, and image-enhanced endoscopy (IEE) have improved the detection rate and diagnostic accuracy of gastric mucosal lesions [5–8], biopsy and histopathological examination are still required for the final diagnosis. Further, the updated Sydney system recommends performing at least five biopsies for the classification and grading of gastritis [9]. However, performing redundant biopsies increases the cost for patients and workload on pathologists in addition to augmenting the associated risks (such as bleeding). Inaccurate biopsies cause misdiagnoses and threaten patient outcomes. Accordingly, precise in vivo histological imaging is highly desirable.

Confocal laser endomicroscopy (CLE) enables real-time in vivo histological observation of gastrointestinal mucosa at the cellular level and realizes "optical biopsy." It aims to overcome the inherent limitations of endoscopic biopsy and reduce the necessity for traditional physical biopsy via optical biopsy [10]. CLE systems can be endoscope-based (no longer commercially available) or probe-based (pCLE). pCLE can pass through the biopsy channel of any standard endoscope and make contact with the mucosa, producing confocal microscopic images with magnification up to × 1000. Our previous studies have proven the high effectiveness of CLE in diagnosing GIM, GIN, and gastric cancer [11–14]. In addition, pCLE significantly reduces the number of biopsies and increases the diagnostic yield of these lesions [14]. However, its image interpretation requires histopathological expertise, and endoscopists vary widely in skill and experience, which affects its clinical applicability and generalizability [15, 16]. Therefore, the application of pCLE has been restricted to some academic centers.

Artificial intelligence (AI) provides an opportunity to address this issue. AI methods, particularly deep-learning algorithms, have been applied for identifying gastric mucosal lesions [17–29]; however, most AI algorithms can provide only dichotomous diagnoses such as detecting whether a lesion is cancerous or non-cancerous. To date, no study has applied AI for the whole-chain diagnosis of Correa cascade in real clinical settings. In addition, no AI program has been developed for pCLE diagnosis of gastric mucosal lesions. In this study, we developed a pCLE computer-aided diagnostic system (CCADS) that can realize real-time whole-chain diagnosis of Correa cascade, and assessed it via multistep validation.

Methods

Study design

This diagnostic study was conducted at Qilu Hospital of Shandong University. CCADS was developed using deep learning networks. Retrospective pCLE images and videos were collected for the development, verification, and testing of CCADS. The multistep validation phase included offline validation (image and video recognition test) and real-time validation (a prospective study). The prospective study was conducted to compare the real-time diagnostic performance of CCADS with that of pCLE experts in a clinical setting. This study was approved by the Ethics Committee of Qilu Hospital of Shandong University (No. 2018(129)) and conducted in accordance with the Declaration of Helsinki. It was registered at https://clinicaltrials.gov/ (NCT03784209).

Collection and preprocessing of images and offline videos

Gastric pCLE videos from February 1, 2015, to July 31, 2017, were reviewed and transformed into single-frame images. Images with typical pCLE features of normal gastric mucosa, inflammation (without atrophy), atrophy, GIM, LGIN, HGIN/CA, and unqualified images were

selected and labeled. Gastric cancer and HGIN were considered under a single category because they are difficult to distinguish using pCLE and should be biopsied [13]. Unqualified images refer to pCLE images with invisible tissue structures, too dark or bright visuals, or artifacts. pCLE examinations may produce unqualified images because rapid probe movements or gastric peristalsis during imaging may create artifacts. Additionally, prolonged examination time causes decreased fluorescein in blood vessels and tissues, potentially resulting in images that are too dark to clearly observe tissue structures. These unqualified images may lead to misdiagnosis. Images were processed using deduplication software we developed to exclude highly similar frames. Videos from August 1, 2017, to December 31, 2017, were selected and edited into video segments; each short video contained images from the time the probe touched the mucosa until the time it was removed. Videos from January 1, 2018, to May 31, 2018, were selected and marked for the offline video recognition test. The most severe histological abnormality in each video was used as the diagnosis. All images and videos were selected and marked according to the diagnostic criteria of pCLE [16] by two experienced endoscopists who had performed over 1000 pCLE procedures; they were verified by another senior expert endoscopist. Histologic diagnosis was the gold standard for labeling. Disagreements in diagnoses were resolved through discussion, failing which the related images or videos were discarded.

Overall, 5771 pCLE examinations were retrospectively collected. A total of 58,901 images from 5139 patients were obtained after deduplication and selection. Finally, 41,743 images were used as the training set, 5719 as the validation set, and 11,439 as the test set. In addition, 461 video segments from 74 patients were collected to train the video recognition ability, and videos of 667 lesions from 558 patients were used for off-line video testing. The characteristics of these images and videos are shown in Additional file 1: Table S1. Images or videos in the training and test sets were selected from different patients.

Development of CCADS

CCADS was constructed using three sub-modules: quality judgment, image recognition, and video diagnosis network (Fig. 1). The quality judgment network was a two-layer convolutional neural network that could distinguish qualified images from unqualified ones. Several neural network modules were evaluated and compared for classifying the pCLE images (Additional file 1: Table S2). Inception-ResNet V2 [30] demonstrated the best diagnostic ability and was selected for image recognition. The input of this network was a pCLE image, and the outputs were diagnostic result and probability. A four-layer fully connected neural network was used to implement the diagnosis of the video. The inputs were the AI diagnosis and diagnostic probability of each extracted image in a video, and the output was the

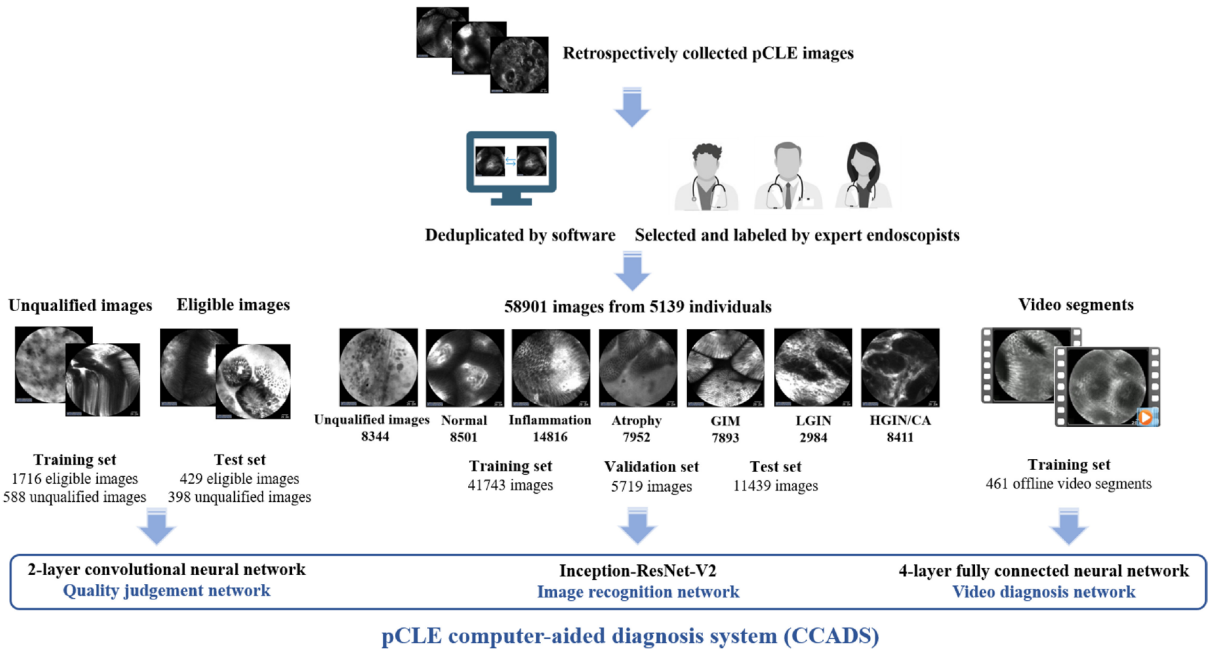


Fig. 1 Workflow diagram for the development of CCADS

diagnosis of the video. The video recognition procedure of CCADS is shown in Additional file 1: Fig. S1. During the pCLE examination, the real-time diagnoses of the present image and video were displayed on the screen (Fig. 2 and Additional file 2: Video S1).

Two practical AI-assisted functions were developed to improve the operability and efficiency of pCLE procedures: automatic image capture and AI-guided targeted biopsy. During the pCLE examination, CCADS automatically captured the pCLE images with high diagnostic probability and saved them in the workstation for further review. The corresponding WLE images were captured simultaneously and matched exactly with the pCLE images (Fig. 3). The endoscopists could determine the precise location to obtain the targeted biopsies by referring to the images.

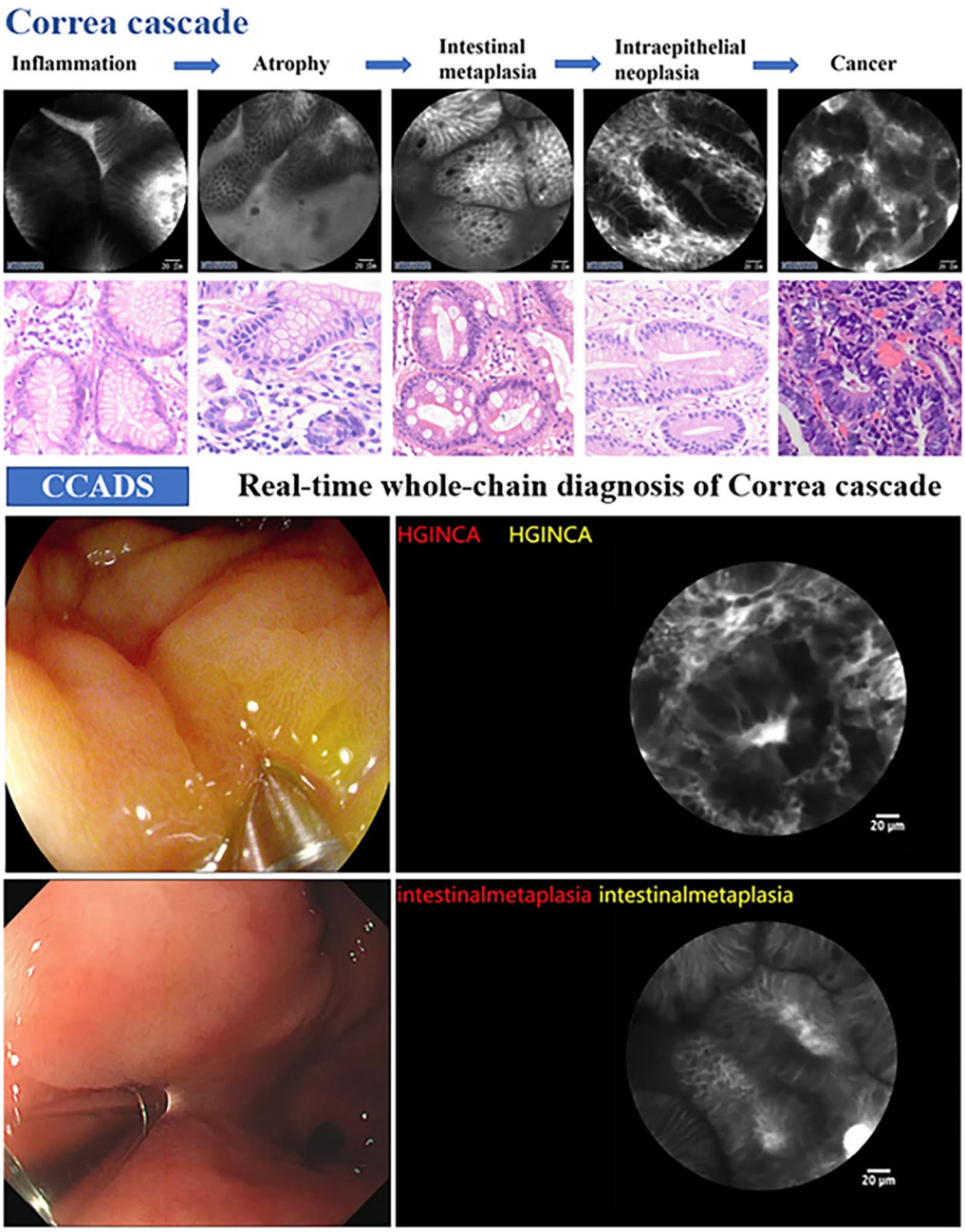


Fig. 2 Whole-chain diagnosis of the Correa cascade by CCADS

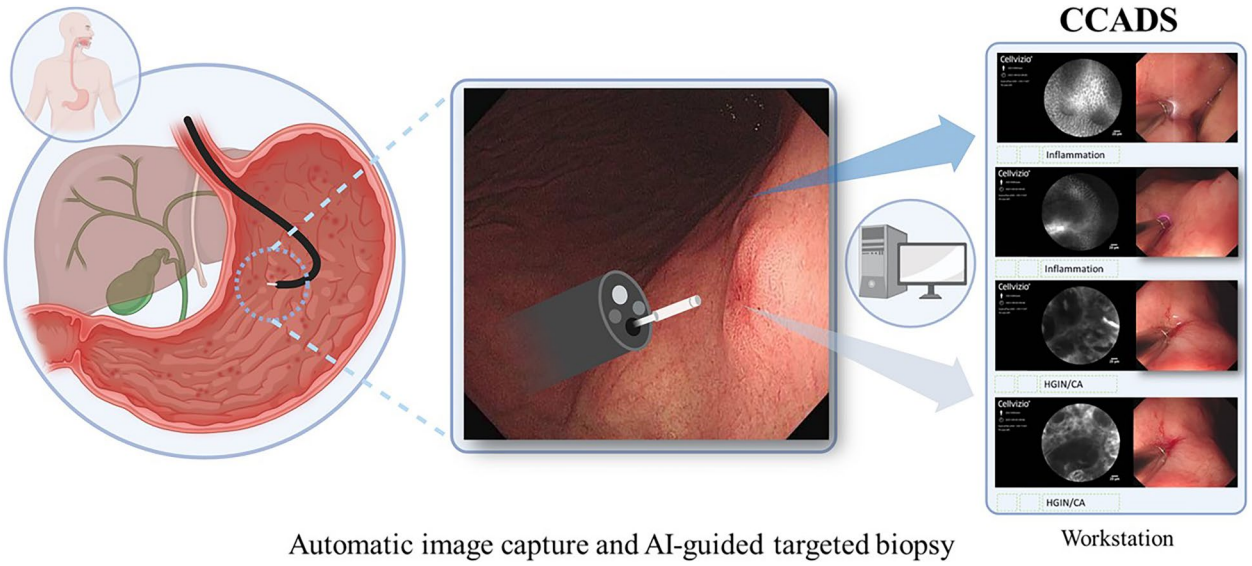


Fig. 3 AI-assisted functions of CCADS

Offline validation of CCADS

Before the prospective study, offline tests, including image and video recognition, were performed to ensure the diagnostic reliability of CCADS. First, we evaluated the ability of CCADS to classify the pCLE images in the test set. Then, selected offline videos were played on the pCLE equipment to simulate the real-time examination and test video recognition. Based on the satisfactory results of these tests, a prospective study was conducted.

Real-time validation of CCADS

Patients

Between October 2019 and September 2021, consecutive patients undergoing upper gastrointestinal pCLE examination at Qilu Hospital of Shandong University were prospectively enrolled. Patients aged 18–80 years who provided written informed consent were included. Patients who were unsuitable for undergoing pCLE, such as those who were pregnant or breastfeeding or those with coagulopathy, impaired renal or hepatic function, known allergy to fluorescein sodium, inability to provide informed consent, no gastric mucosal lesion found in WLE, and lesion with pathologic diagnosis not included in non-atrophic gastritis, atrophic gastritis, GIM, LGIN, and HGIN/CA such as lymphoma were excluded.

Sample size calculation

The sample size was calculated using PASS15 (NCSS, LLC, Kaysville, USA). According to a previous study, gastric neoplasms can be diagnosed through CLE with a sensitivity of 84.0% and specificity of 92.1% [13]. CCADS could diagnose gastric neoplasms with a sensitivity of 96.23% and specificity of 95.11% in our offline video recognition test. From a national multicenter survey, the prevalence of dysplasia found through endoscopy in China was 7.3% [31]. Based on these data, we assumed that at least 836 participants (including 61 participants with neoplasms) were required, with a statistical power of 0.90 and significance level of 0.05.

Endoscopic procedure

After routine preparation for anesthetic gastroscopy, patients underwent WLE examination, and all lesions were recorded. Fluorescein sodium (0.02 mL/kg, 10%) was administered intravenously. The probe was inserted through the biopsy channel of the endoscope, and pCLE was performed on all macroscopic lesions. Multi-point scanning was performed from the periphery to the center of the lesion. Although the specific number of observation points was not fixed, all areas of the lesion should be examined. At each observation point, the probe remained stationary for a short duration (typically several seconds) to acquire clear and stable video. The observation time for one lesion was not predetermined and depended primarily on the lesion size and the number of observation points. Each lesion was independently diagnosed by the endoscopists using CCADS, and the coordinator recorded these data accordingly. The diagnosis of CCADS was displayed on a separate screen visible only to the study coordinator. The most severe diagnosis obtained by CCADS was taken as the final AI diagnosis. The diagnosis by the endoscopists was based on pCLE and WLE. Since the aim of this study was to evaluate the diagnostic performance of CCADS for the real-time pCLE

examination and compare that with expert endoscopists, the IEE function was not activated to avoid interference with diagnosis. In addition, the endoscopists were blinded to the previous endoscopic and pathological findings of the patients until the diagnosis was recorded. Finally, targeted biopsy was taken from the site where the most severe histological abnormality was observed and sent for histological assessment. The endoscopic procedures were performed by seven expert endoscopists with experience of more than 500 pCLE procedures. Endoscopic examinations were performed using the EG29-i10 endoscope with the EPK-i7000 image processor (Pentax, Tokyo, Japan) or the GIF-HQ290 endoscope with the Evis Lucera Elite CV-290 system (Olympus, Tokyo, Japan); pCLE was performed using the Cellvizio pCLE system (Mauna Kea Technologies, Paris, France).

Histological evaluation

All specimens were sent for histopathological examination and evaluated by experienced pathologists (with more than 5 years of experience). Each specimen was independently reviewed by two pathologists. Disagreements were resolved through discussion. Inflammation, atrophy, and GIM were diagnosed based on the updated Sydney system [9], and neoplasms were diagnosed according to the Vienna classification [32]. If the patient subsequently underwent surgery or endoscopic resection at our hospital, the postoperative pathology was taken as the final histological diagnosis.

Outcomes

The primary outcome was the real-time performance of CCADS in classifying gastric mucosal lesions in the prospective study, including accuracy, sensitivity, specificity, positive predictive value (PPV), and negative predictive value (NPV), with histopathology as the gold standard. The secondary outcome measure was the comparison of diagnostic performance between CCADS and the expert endoscopists in the prospective study.

Statistical analysis

Statistical analysis was performed using NCSS12 (NCSS, LLC, Kaysville, USA). The calculation of accuracy, sensitivity, specificity, PPV, and NPV is based on the comparison of two-category data with the gold standard. Therefore, when we calculated these metrics for one category, such as HGIN/CA, the other diagnoses were taken as one category (non-HGIN/CA). The secondary outcome measure, namely the comparison of diagnostic measurements between CCADS and expert endoscopists, was performed using the chi-square test. Matplotlib [33] was used to obtain the receiver operating characteristic curve. A two-sided *P*-value of < 0.05 was considered statistically significant. All authors have access to the study data and have reviewed and approved the final manuscript.

Results

Overall, 11,439 images and 667 videos were recognized in the off-line test. Between October 2019 and September 2021, 2314 consecutive patients who underwent upper gastrointestinal pCLE examination were invited to participate in the prospective study, of whom 951 patients were enrolled according to the inclusion and exclusion criteria. 1254 lesions (including 443 inflammation, 91 atrophy, 629 GIM, 27 LGIN, and 64 HGIN/CA) were detected. All lesions were analyzable by CCADS. The median total procedure time was 17 min (range 7–45 min), and the median time for pCLE observation was 2.7 min (range 1–11 min). No adverse event (including adverse reaction to intravenous fluorescein sodium administration) was reported. The characteristics of the patients and lesions are presented in Table 1. The validation workflow of CCADS is shown in Fig. 4.

The diagnostic accuracies of CCADS in recognizing images of inflammation, atrophy, GIM, LGIN, and HGIN/CA were 95.05%–99.61% (Additional file 1: Table S3). The area-under-the-curve values of the receiver operating characteristic curve were high (0.9857–0.9998), as shown in Additional file 1: Fig. S2. The accuracies of offline video recognition were 92.80%–98.95% (Additional file 1: Table S4). The real-time diagnostic performances of CCADS and the expert endoscopists are presented in Table 2. The confusion matrices are included in Additional file 1: Table S5–S7. In the prospective study, the accuracies of CCADS for the five categories were 91.71%–97.13%. CCADS achieved a high accuracy of 97.13% (95%CI, 96.05%–97.98%), sensitivity of 98.44% (95%CI, 91.60%–99.96%), and specificity of 97.06% (95%CI, 95.93%–97.94%) in diagnosing HGIN/CA. The sensitivity and NPV of CCADS for HGIN/CA were not significantly different ($p = 0.171$ and 0.188, respectively) compared with those of experts, but its diagnostic accuracy, specificity, and PPV of CCADS were lower ($p = 0.003$, < 0.001, and 0.004, respectively). For LGIN and atrophy, CCADS showed no significant differences in accuracy, sensitivity, specificity, PPV, or NPV compared with the experts. CCADS achieved significantly higher specificity and PPV ($p = 0.004$ and 0.006, respectively) for GIM, while maintaining similar accuracy, sensitivity, and NPV.

Notably, CCADS identified gastric neoplasms (LGIN + HGIN/CA) with significantly higher sensitivity (96.70% (95%CI, 90.67%–99.31%) vs. 89.01% (95%CI, 80.72%–94.60%); $p = 0.044$) than the experts, though their accuracies, specificities, PPVs, and NPVs did not

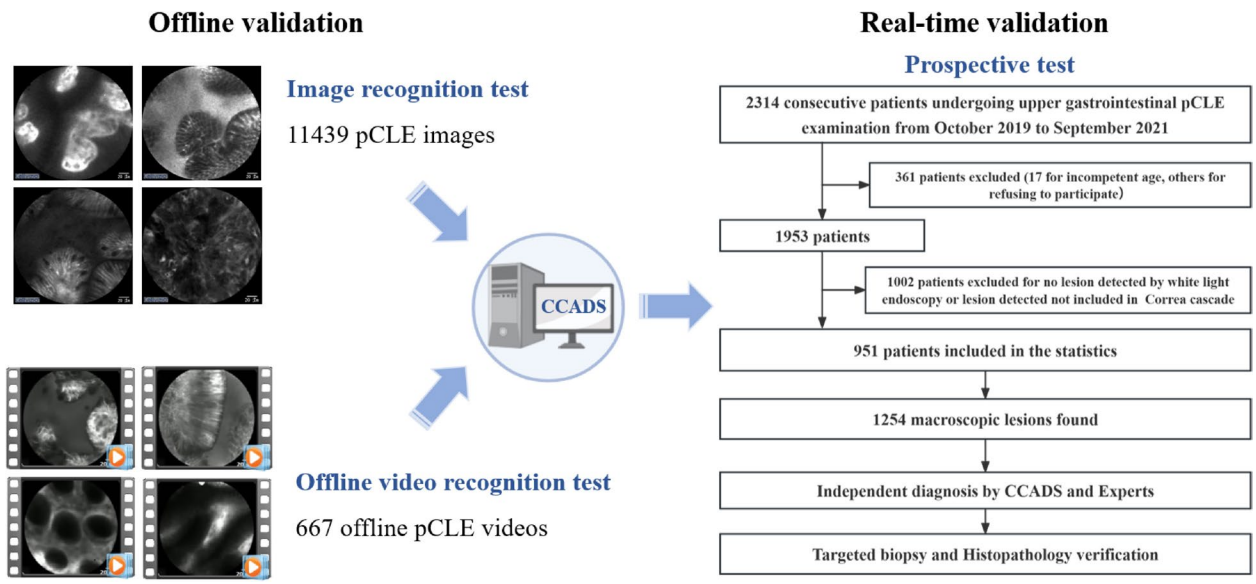


Fig. 4 Workflow diagram for the validation of CCADS

Table 1 Baseline characteristics of patients and lesions

Patients, *n*	**951**
Sex	
Male, *n* (%)	562 (59.1%)
Female, *n* (%)	389 (40.9%)
Age, mean (range), years	55.57 (22–80)
Macroscopic lesions, *n*	1254
Lesion size, mean (range), cm	0.9 (0.2–6.0)
Number of biopsies per patient, *n*	1.8
Number of biopsies per lesion, mean (range), *n*	1.4, (1–7)
Histological diagnosis, *n*	
Inflammation	443
Atrophy	91
GIM	629
LGIN	27
HGIN/Ca	64
Locations, *n*	
Cardia	94
Fundus	48
Body	266
Angle	206
Antrum	612
Pylorus	24
Anastomotic stoma	4

differ significantly. Additionally, CCADS misdiagnosed only three LGIN cases as non-neoplastic lesions, whereas the experts misdiagnosed nine LGIN cases and one HGIN case.

Discussion

In this study, we developed the first pCLE computer-aided diagnostic system named CCADS for diagnosing the Correa cascade of gastric cancer and evaluated its effectiveness via multistep validation. CCADS achieved high diagnostic performance in the image test, video test, and a prospective diagnostic study with the largest sample size in the field of pCLE by far. To the best of our knowledge, CCADS is the first AI program that can implement a whole-chain diagnosis of the Correa cascade and realize in vivo histological evaluation for the stomach in a real clinical setting worldwide.

Endoscopists vary widely in skills and experience, which can lead to misdiagnoses and threaten patient outcomes. Several effective AI programs have been applied to improve this situation. For instance, ENDOANGEL is an AI-powered system compatible with various endoscopic devices and has been proven effective through multiple studies and clinical applications. It can improve the quality of endoscopic examinations by reducing blind spots and implementing quality control [19]. Additionally, this system can detect focal lesions and lower the miss rate of gastric neoplasms using WLE [20], as well as identify gastric precancerous conditions through IEE [21]. Furthermore, it can delineate the margins of early gastric cancer and predict invasion depth and differentiation status using ME-IEE [22]. Evolving beyond conventional AI, ENDOANGEL now integrates the feature extraction-based logical anthropomorphic diagnostic system [23], explainable AI incorporated with domain knowledge [24], and multi-modal data synthesis [25],

Table 2 Performance comparison between CCADS and the endoscopists in the prospective test

Group	CCADS					Expert				
	Accuracy (95% CI)	**Sensitivity (95% CI)**	**Specificity (95% CI)**	**PPV (95% CI)**	**NPV (95% CI)**	**Accuracy (95% CI)**	**Sensitivity (95% CI)**	**Specificity (95% CI)**	**PPV (95% CI)**	**NPV (95% CI)**
Inflammation	92.34 (90.73–93.76)	82.39 (78.52–85.83)	97.78 (96.51–98.68)	95.30 (92.67–97.19)	91.04 (88.95–92.86)	89.95 (88.15–91.56)	79.68 (75.63–83.33)	95.56 (93.91–96.87)	90.75 (87.42–93.43)	89.60 (87.37–91.55)
Atrophy	93.86 (92.39–95.12)	72.53 (62.17–81.37)	95.53 (94.18–96.64)	55.93 (46.50–65.06)	97.8 (96.77–98.57)	92.58 (90.99–93.97)	60.44 (49.64–70.54)	95.10 (93.70–96.27)	49.11 (39.54–58.73)	96.85 (95.66–97.78)
GIM	91.71 (90.04–93.17)	86.96 (84.08–89.50)	96.48 (94.72–97.78)	96.13 (94.20–97.56)	88.03 (85.36–90.37)	89.87 (88.07–91.49)	86.96 (84.08–89.50)	92.80 (90.48–94.70)	92.40 (89.96–94.40)	87.61 (84.86–90.03)
LGIN	94.18 (92.74–95.41)	74.07 (53.72–88.89)	94.62 (93.21–95.82)	23.26 (14.82–33.61)	99.4 (98.77–99.76)	93.22 (91.69–94.55)	59.26 (38.80–77.61)	93.97 (92.49–95.24)	17.78 (10.52–27.26)	99.05 (98.32–99.53)
HGIN/Ca	97.13 (96.05–97.98)	98.44 (91.60–99.96)	97.06 (95.93–97.94)	64.29 (53.97–73.71)	99.91 (99.52–100)	98.8 (98.03–99.33)	93.75 (84.76–98.27)	99.08 (98.35–99.54)	84.51 (73.97–92.00)	99.66 (99.14–99.91)
Neoplasm	92.11 (90.47–93.54)	96.70 (90.67–99.31)	91.75 (90.01–93.26)	47.83 (40.42–55.30)	99.72 (99.18–99.94)	92.82 (91.25–94.19)	89.01 (80.72–94.60)	93.12 (91.51–94.51)	50.31 (42.33–58.28)	99.09 (98.32–99.56)
P-value	Accuracy	Sensitivity	Specificity	PPV	NPV					
Inflammation	0.035*	0.304	0.013*	0.013*	0.307					
Atrophy	0.204	0.084	0.624	0.300	0.160					
GIM	0.112	1.000	0.004*	0.006*	0.816					
LGIN	0.324	0.248	0.486	0.368	0.341					
HGIN/Ca	0.003 *	0.171	< 0.001*	0.004*	0.188					
Neoplasm	0.496	0.044*	0.210	0.645	0.056					

*$p < 0.05$

thereby advancing AI diagnosis into a multidimensional, interpretable area. Unlike the rapid advancement of AI in WLE and IEE, AI research in pCLE is still limited. An AI system named iCLE demonstrated high diagnostic performance for esophageal squamous neoplasia in a prospective study and significantly improved accuracy and sensitivity for non-expert endoscopists [26]. Another deep learning model achieved human-level accuracy in diagnosing dysplasia in Barrett's esophagus [27]. Additionally, an AI algorithm for pCLE images of colonic polyps showed comparable performance to expert endoscopists while outperforming junior endoscopists [28]. Beyond in vivo applications, an AI-driven model successfully identified gastric cancer tissue in ex-vivo samples using confocal laser endomicroscopy and could be a complementary tool for pathologists [29]. However, prior to CCADS, no AI system had been developed for real-time in vivo pCLE diagnosis of gastric mucosal lesions.

Compared with dichotomous diagnoses, whole-chain diagnosis of Correa cascade is more conducive to fully estimating the risk of gastric cancer, developing individualized follow-up strategies, and achieving early detection of gastric neoplasms. To realize this aim and produce a fully automated algorithm, we used pCLE as the target for AI analysis. pCLE could present the microscopic structure of gastric pits, microvasculars, and epithelial cells, and enable in vivo histological evaluation for gastrointestinal lesions. It could be used combined with other endoscopic equipments such as WLE or IEE. Moreover, its operation is convenient and feasible for general endoscopists. Endoscopists could perform an optical biopsy by touching the probe to the mucosa, similar to taking a conventional biopsy. However, interpretation of pCLE images requires histopathological knowledge and much experience, which restricts its application among general endoscopists. Subjective differences in diagnosis impact the reliability of optical biopsy. How to reduce the difficulty of pCLE image interpretation and provide objective referential diagnosis is the most necessary problem to be solved for CLE technology. CCADS fills this gap and innovatively provides a comprehensive diagnostic system, including lesion identification and operational assistance.

CCADS significantly improved the diagnostic sensitivity of gastric neoplasms, which is vital for the screening and treatment of early gastric cancer. CCADS effectively reduced the misdiagnoses of neoplasms. In the identification of HGIN/CA, it showed a higher sensitivity than experts, although the difference was not significant ($p=0.171$). Further, although the diagnostic accuracy and specificity of CCADS were lower than those of experts, they were relatively high in the clinical setting. Moreover, it is the only reported AI program that can distinguish LGIN with a high accuracy of 94.18%. In addition, a previous study has demonstrated that pCLE can provide precise margin delineation of early gastric cancer for endoscopic submucosal dissection (ESD) [34], so CCADS may be helpful in determining the lateral margin of ESD, especially for flat lesions that are not well displayed using chromoendoscopy.

CCADS has also shown well diagnostic performance in identifying gastric precancerous conditions and is therefore expected to be suitable for evaluating gastritis stages. The updated Sydney system recommends at least five biopsies from standardized regions for histopathological staging of gastritis. The operative link for gastritis assessment (OLGA) and the operative link on gastric intestinal metaplasia assessment (OLGIM) staging systems have been proposed for the staging of atrophy and GIM, and proven to be effective in risk estimation of gastric cancer [35]. Compared with standard biopsies according to the updated Sydney system, real-time pCLE combined with targeted biopsies by experts could improve the diagnostic yield while reducing biopsy sampling [14]. Since CCADS provides reliable real-time diagnosis, general endoscopists can perform efficient and comprehensive screening of the stomach. Automatic OLGA and OLGIM based on optical biopsy might be realized using CCADS, which would be evaluated in further study. With the assistance of CCADS, pCLE can be used as an effective and easy-to-use screening and surveillance modality for gastric neoplasms and precancerous conditions.

The innovative AI-assisted functions of CCADS had the potential to improve the objectivity of pCLE diagnosis and the precision of targeted biopsy. Because pCLE images move rapidly during the examination, endoscopists (even experts) may miss some images when performing endoscopy. Although they can watch video playback for remedies, it is time-consuming. CCADS can automatically capture pCLE images with high diagnostic probabilities and save them in the workstation for review, thereby reducing subjective diagnostic errors caused by missing images. Moreover, locating the exact biopsy site of a suspicious lesion recognized by pCLE is challenging when multiple lesions are present in the same scanned area. In some cases, it may be difficult to determine whether the biopsy sample was obtained from the most severe part of the lesion or from the adjacent mucosa. AI-guided targeted biopsy can capture and match the pCLE images and corresponding WLE images automatically. The exact position of the lesion observed in pCLE could be located from the WLE image showing where the probe touched the mucosa. Endoscopists can identify the exact location for biopsy by referring to the images. Thus, a point-to-point targeted biopsy can be assured.

Since CCADS can assist endoscopists in making accurate real-time diagnoses and performing precisely targeted biopsies, it helps minimize the need for biopsies. In traditional gastroscopy, redundant biopsies are collected from lesions that are subsequently proven to be non-neoplastic, which increases the workload on pathologists and imposes higher costs on patients. Moreover, accurate biopsy is essential in selecting an appropriate resection method for neoplastic lesions; traditional non-targeted biopsy may misjudge the characteristics of the lesion, which can result in inappropriate management. General endoscopists often require multiple biopsies to ensure histopathological accuracy, which may cause submucosal fibrosis and complicate subsequent ESD. The deficiencies of traditional endoscopic biopsy could be overcome by using CCADS-assisted pCLE. As endoscopists were blinded to AI diagnoses in the study design, this study could not directly quantify the biopsy reduction attributable to CCADS. Nevertheless, prior research has proved pCLE's capacity to reduce biopsy needs. In a randomized controlled trial enrolling patients undergoing surveillance for GIM, GIN, or EGC, the number of biopsy samples in the pCLE group (3.5) was significantly lower than that in the standard biopsy group (6.8), representing a 45% reduction [14]. Our findings confirm that CCADS achieves high accuracy and reliability, and could provide trustworthy reference diagnoses for non-expert endoscopists. This system could lower the difficulty of pCLE utilization, enabling endoscopists of varying expertise levels to effectively use it. Consequently, CCADS facilitates the transition from traditional physical biopsy to optical biopsy combined with targeted biopsy.

Histopathological examination is a costly procedure, and reducing biopsy samples may decrease patient expenses; however, pCLE systems also involve considerable costs. According to the ASGE technology status evaluation report, the Cellvizio 100 Series equipment and GastroFlex UHD probe used in this study were priced at USD 175,000 and USD 9200, respectively [15]. The reusable probe is validated for 100 examination procedures (30 min per procedure). Cost-effectiveness depends on comparing histopathology costs with pCLE expenses, which vary regionally. Overall, the economic benefit is determined by the extent to which pCLE can reduce biopsy requirements. In high-risk populations for gastric cancer (e.g., patients with atrophy), who typically require more biopsies for gastritis staging or lesions confirmation, pCLE may reduce overall costs by minimizing unnecessary biopsies through optical biopsy evaluation and targeted biopsy. Conversely, for non-high-risk populations or patients not typically requiring biopsies, the economic benefit of pCLE is limited. Therefore, implementing risk stratification to identify the patients most likely to benefit from pCLE could optimize its cost-effectiveness. Moreover, reducing biopsies holds significance beyond cost savings. It decreases biopsy-related complications and minimizes interference with subsequent endoscopic therapies.

Due to its high magnification (up to 1000×), pCLE has a limited field of view, making lesion detection primarily dependent on WLE and IEE. Although pCLE based on WLE proved effective and IEE was not activated in this study to avoid interference with the diagnosis, the combination of IEE and CCADS-assisted pCLE could be practical in clinical settings. IEE can serve as a red-flag technique to identify suspicious lesions, while pCLE provides histological diagnosis for these lesions. Considering the high NPVs of CCADS, especially for neoplasm (99.72%), a diagnostic and biopsy strategy may be effective for general endoscopists. After observation with WLE and IEE (if available), pCLE is used to examine suspected lesions and screen the five standardized gastric regions. If a lesion is diagnosed as LGIN or HGIN/CA by CCADS, a targeted biopsy should be performed with AI guidance. If atrophic gastritis or GIM is diagnosed, biopsy is not required unless the endoscopist shows concerns. If only inflammation is present, biopsy is unnecessary. This strategy will be assessed in further study.

Magnifying endoscopy is a commonly used technique for optical diagnosis and obtaining targeted biopsies. ME demonstrates high sensitivity and specificity for gastric neoplasms and precancerous conditions. However, there is still a lack of large-sample studies comparing the clinical application value of ME and pCLE. Only one study compared the diagnostic efficacy of ME-IEE alone versus ME-IEE combined with pCLE for intestinal metaplasia, proving that ME-IEE followed by pCLE had higher sensitivity and PPV [36]. The diagnostic interpretation and operation of ME present challenges for non-expert endoscopists. AI programs can effectively assist non-expert endoscopists in diagnosis [22]. However, in terms of operation, the use of ME-IEE requires endoscopists to precisely adjust the focal length of the endoscope and the distance from the mucosa to obtain clear images, which demands high skill in endoscopic control. In contrast, the operation of pCLE is simpler. Endoscopists can perform optical biopsy by placing the probe on the mucosal surface, with a technical difficulty level similar to taking biopsies. Therefore, we speculate that experts would achieve excellent diagnostic performance with either ME or CCADS-aided pCLE, whereas for endoscopists with limited technical skills, the latter might be easier to use. Further research is needed to compare CCADS-aided pCLE with other equipment.

The time required for pCLE examination and AI identification is a crucial factor affecting the clinical application

of CCADS. The median total procedure time in this study is 17 min (range 7–45 min), consistent with a previous study (17 min; range 11–31 min) that proved pCLE examination did not significantly prolong the procedure duration compared with standard biopsies [14]. We did not directly assess whether CCADS would increase procedural duration because endoscopists were blinded to the AI diagnosis. However, as illustrated in Additional file 1: Fig. S1, CCADS generates a video diagnosis by extracting and evaluating 10 frames of pCLE video per second, enabling real-time diagnostic output within 1 s. In clinical practice, CCADS demonstrates rapid recognition speed—once stable images are obtained, the AI delivers an immediate diagnosis, as shown in Additional file 2: Video S1. Thus, CCADS would not prolong the overall examination time and has good usability.

The characteristics of pCLE images introduce uniqueness and challenges for CCADS in image recognition compared to other computer aided diagnosis (CAD) systems. First, CCADS recognizes planar histological images, whereas other endoscopic CAD systems identify the overall morphology of lesions, which may be affected by distance, angle, and light intensity. Second, pCLE images are monochrome rather than in color, reducing the complexity of image recognition but also diminishing the identifiable lesion features. Third, the high magnification of pCLE results in a narrower field of view per frame, which facilitates AI analysis. However, probe movement and gastric peristalsis may introduce artifacts that impact image quality. pCLE is more significantly affected by such artifacts compared to WLE or IEE, presenting challenges for AI recognition.

To address the distinctive characteristics of pCLE images and to improve the image recognition capability, we implemented the following measures. First, this study utilizes a large-sample training set, which helps AI comprehensively learn the characteristics of pCLE images. The prospective evaluation involves the largest prospective trial in the field of pCLE to date and assures the system's generalizability in real-world settings. Second, innovative procedures, including the deduplication of images and recognition of unqualified images, were used to control the biases. We designed a software program to recognize and discard highly similar images in the training set that might cause overfitting of the neural network or reduce its generalizability, which decreased the selection bias. Generally, researchers select typical and distinct images and exclude unqualified ones to minimize interference during AI identification. Nevertheless, if unqualified images cannot be identified, they may be incorrectly categorized, resulting in misdiagnosis in a real clinical setting. The quality judgment network was specially designed and trained using unqualified images. Therefore, it could effectively identify unqualified images in videos, reducing their impact on diagnosis as much as possible.

The Inception-ResNetV2 algorithm used in this study achieves outstanding performance in image classification by integrating the multi-scale feature extraction of Inception modules with the residual connections from ResNet. During CCADS development, Inception-ResNetV2 exhibited superior diagnostic accuracy among all tested architectures. With recent advancements in deep learning, emerging algorithms could further improve the performance of AI for pCLE. Vision Transformers (ViTs) and their derivatives leverage self-attention mechanisms to model long-range dependencies, enhancing their suitability for dynamic endoscopic video analysis and potentially improving diagnostic sensitivity. Meanwhile, architectures like EfficientNetV2 combine neural architecture search (NAS) with manual scaling to achieve superior computational efficiency. Hybrid approaches (e.g., ConvNeXt) and dynamic networks (e.g., DynamicViT) can handle diverse or complex images, making them effective for diagnosing pCLE images. Multimodal AI models can further improve accuracy by integrating WLE, IEE, and CLE features to analyze lesions across macroscopic and microscopic scales. Explainable AI techniques can interpret histopathological features in pCLE images, thereby improving diagnostic reliability and endoscopist confidence. Although implementing these algorithms may require adjustments to model architectures and preprocessing pipelines, they have the potential to improve the diagnostic accuracy and interpretability of pCLE images.

Limitations

This study has some limitations. First, all endoscopic procedures in this study were performed by experienced pCLE specialists. Experts can detect lesions more quickly and obtain high-quality pCLE images, which aids AI recognition. This ensured high accuracy of targeted biopsies and reduced the potential selection bias. However, in routine clinical practice, non-expert endoscopists' lower operational stability may compromise image quality, potentially resulting in inferior diagnostic performance of CCADS. Additionally, non-experts may encounter challenges in achieving precise targeted biopsies. Although we have designed the AI-assisted targeted biopsy function to improve biopsy accuracy and performed specialized training to address unqualified images, the actual performance of CCADS when operated by non-experts requires further validation. Second, although the superior diagnostic performance of CCADS was demonstrated, its effectiveness as an assistive system for expert and non-expert endoscopists was not evaluated. Third, comparisons between non-expert endoscopists and CCADS were

not performed in this study; as the diagnostic capability of CCADS is comparable to that of experts, its diagnostic efficiency should be superior to that of non-expert endoscopists. Finally, this was a single-center study.

Conclusions

CCADS provides an innovative, comprehensive solution for the whole-chain optical diagnosis of Correa cascade of gastric cancer. It has the potential to assist endoscopists in the application of pCLE, optimize the surveillance of gastric neoplasms and precancerous conditions, and reduce unnecessary biopsies.

Abbreviations

AI	Artificial intelligence
CAD	Computer aided diagnosis
CCADS	PCLE computer-aided diagnosis system
CLE	Confocal laser endomicroscopy
eCLE	Endoscope-based confocal laser endomicroscopy
GIM	Gastric intestinal metaplasia
HGIN	High-grade intraepithelial neoplasia
LGIN	Low-grade intraepithelial neoplasia
pCLE	Probe-based confocal laser endomicroscopy
PPV	Positive predictive value
NPV	Negative predictive value

Supplementary Information

The online version contains supplementary material available at https://doi.org/10.1186/s12916-025-04310-9.

Additional file 1. Table S1–S6. Table S1- [The characteristics of the training, validation, and test sets for pCLE images, and training and off-line test sets for pCLE videos]. Table S2- [Performances of several alternative neural network modules for the classification of pCLE images]. Table S3- [Diagnostic performance of CCADS in the image recognition test]. Table S4- [Diagnostic performance of CCADS in the offline video recognition test]. Table S5- [Confusion matrix of CCADS in the image recognition test]. Table S6- [Confusion matrix of CCADS in the offline video recognition test]. Table S7- [Confusion matrixes of CCADS and experts in the prospective test].Figures S1–S2. Fig. S1- [Workflow diagram for the video recognition procedure of CCADS]. Fig. S2- [Receiver operating characteristic curve of CCADS when recognizing pCLE images]..

Additional file 2. Video S1- [Real-time diagnostic performance of CCADS] This video includes two cases recorded during routine pCLE examinations and demonstrates the performance of CCADS in the diagnosis of gastric mucosal lesions. The real-time diagnosis of the video (red words) and present image (yellow words) during the pCLE procedure are displayed on the screen (the top left corner of the picture). Although CCADS could not diagnose every image correctly, it could calculate the AI diagnosis and diagnostic probability of each image in a video and provide an accurate diagnosis of the video. Case 1 shows the recognition performance of the CCADS for gastric neoplasm. A lesion on the angle was found, and CCADS provided real-time diagnosis (HGIN/CA); this was then followed by the histopathological diagnosis of the ESD specimen. Case 2 shows the recognition performance of CCADS for gastric precancerous conditions. White-light endoscopy revealed atrophic gastritis, and pCLE screening was performed. Although the pCLE images moved quickly and peristalsis of the stomach interfered with the observation, CCADS was able to accurately recognize the intestinal metaplasia and atrophy at different regions of the stomach. It could realize the automatic and complete assessment of gastritis stages without the need for biopsy.

Acknowledgements

Not applicable.

Authors' contribution

Y.L., X.Z., and Z.L. conceived, designed, and supervised the study; Z.L. verified data labeling and edited the manuscript. GQ. L. and GC. L. performed data collection and labeling, analyzed the results, and drafted and edited the manuscript; X.S. provided technical support for the algorithm and methodology development; and R.J. provided guidance during data labeling, study design, and manuscript editing. T.M., Y.Z., Y.H., and X.Y. contributed to data collection. J.S, Q.Q., and J.G. contributed to data analysis and manuscript editing. All authors read and approved the final manuscript.

Funding

This study was funded by the Key Research and Development Program of Shandong Province (2021CXGC010506); National Natural Science Foundation of China (81873550 and 82070552); Taishan Scholars Program of Shandong Province; and Natural Science Foundation of Shandong Province (ZR2020LZL003).

Data availability

pCLE images and videos are not publicly available to protect patient privacy. Other data are available from the corresponding author on reasonable request.

Declarations

Ethics approval and consent to participate

This study was approved by the Ethics Committee of Qilu Hospital of Shandong University [No. 2018(129)] and conducted in accordance with the Declaration of Helsinki. All participants signed informed consent forms.

Consent for publication

Not applicable.

Competing interests

The authors declare no competing interests.

Author details

[1]Department of Gastroenterology, Qilu Hospital of Shandong University, 107 Wenhuaxi Road, Jinan, Shandong 250012, China. [2]Laboratory of Translational Gastroenterology, Qilu Hospital of Shandong University, Jinan, Shandong, China. [3]Robot Engineering Laboratory for Precise Diagnosis and Therapy of GI Tumor, Qilu Hospital of Shandong University, Jinan, Shandong, China. [4]Qingdao Medicon Digital Engineering Co., Ltd, Qingdao, Shandong, China.

Received: 18 June 2024 Accepted: 30 July 2025
Published online: 30 September 2025

References

1. Bray F, Ferlay J, Soerjomataram I, Siegel RL, Torre LA, Jemal A. Global cancer statistics 2018: GLOBOCAN estimates of incidence and mortality worldwide for 36 cancers in 185 countries. CA Cancer J Clin. 2018;68(6):394–424.
2. Correa P. Human gastric carcinogenesis: a multistep and multifactorial process—first American Cancer Society award lecture on cancer epidemiology and prevention. Cancer Res. 1992;52(24):6735–40.
3. Pimentel-Nunes P, Dinis-Ribeiro M, Ponchon T, et al. Endoscopic submucosal dissection: European society of gastrointestinal endoscopy (ESGE) guideline. Endoscopy. 2015;47(9):829–54.
4. Carpenter HA, Talley NJ. Gastroscopy is incomplete without biopsy: clinical relevance of distinguishing gastropathy from gastritis. Gastroenterology. 1995;108(3):917–24.
5. Anagnostopoulos GK, Yao K, Kaye P, et al. High-resolution magnification endoscopy can reliably identify normal gastric mucosa, Helicobacter pylori-associated gastritis, and gastric atrophy. Endoscopy. 2007;39(3):202–7.

6. Dinis-Ribeiro M, da Costa-Pereira A, Lopes C, et al. Magnification chromoendoscopy for the diagnosis of gastric intestinal metaplasia and dysplasia. Gastrointest Endosc. 2003;57(4):498–504.
7. Pimentel-Nunes P, Dinis-Ribeiro M, Soares JB, et al. A multicenter validation of an endoscopic classification with narrow band imaging for gastric precancerous and cancerous lesions. Endoscopy. 2012;44(3):236–46.
8. Kato M, Kaise M, Yonezawa J, et al. Magnifying endoscopy with narrow-band imaging achieves superior accuracy in the differential diagnosis of superficial gastric lesions identified with white-light endoscopy: a prospective study. Gastrointest Endosc. 2010;72(3):523–9.
9. Dixon MF, Genta RM, Yardley JH, Correa P. Classification and grading of gastritis: the updated Sydney system. Am J Surg Pathol. 1996;20(10):1161–81.
10. Wang KK, Carr-Locke DL, Singh SK, et al. Use of probe-based confocal laser endomicroscopy (pCLE) in gastrointestinal applications. A consensus report based on clinical evidence. United Eur Gastroenterol J. 2015;3(3):230–54.
11. Li Z, Zuo XL, Yu T, et al. Confocal laser endomicroscopy for in vivo detection of gastric intestinal metaplasia: a randomized controlled trial. Endoscopy. 2014;46(4):282–90.
12. Li Z, Yu T, Zuo XL, et al. Confocal laser endomicroscopy for in vivo diagnosis of gastric intraepithelial neoplasia: a feasibility study. Gastrointest Endosc. 2010;72(6):1146–53.
13. Li WB, Zuo XL, Li CQ, et al. Diagnostic value of confocal laser endomicroscopy for gastric superficial cancerous lesions. Gut. 2011;60(3):299–306.
14. Zuo XL, Li Z, Li CQ, et al. Probe-based endomicroscopy for in vivo detection of gastric intestinal metaplasia and neoplasia: a multicenter randomized controlled trial. Endoscopy. 2017;49(11):1033–42.
15. ASGE Technology Committee. Confocal laser endomicroscopy. Gastrointest Endosc. 2014;80(6):928–38.
16. Li Z, Zuo XL, Li CQ, et al. New classification of gastric pit patterns and vessel architecture using probe-based confocal laser endomicroscopy. J Clin Gastroenterol. 2016;50(1):23–32.
17. Luo H, Xu G, Li C, et al. Real-time artificial intelligence for detection of upper gastrointestinal cancer by endoscopy: a multicentre, case-control, diagnostic study. Lancet Oncol. 2019;20(12):1645–54.
18. Cho BJ, Bang CS, Park SW, et al. Automated classification of gastric neoplasms in endoscopic images using a convolutional neural network. Endoscopy. 2019;51(12):1121–9.
19. Wu L, Zhou W, Wan X, et al. A deep neural network improves endoscopic detection of early gastric cancer without blind spots. Endoscopy. 2019;51(6):522–31.
20. Wu L, Shang R, Sharma P, et al. Effect of a deep learning-based system on the miss rate of gastric neoplasms during upper gastrointestinal endoscopy: a single-centre, tandem, randomised controlled trial. Lancet Gastroenterol Hepatol. 2021;6(9):700–8.
21. Xu M, Zhou W, Wu L, et al. Artificial intelligence in the diagnosis of gastric precancerous conditions by image-enhanced endoscopy: a multicenter, diagnostic study (with video). Gastrointest Endosc. 2021;94(3):540–8.
22. Ling T, Wu L, Fu Y, et al. A deep learning-based system for identifying differentiation status and delineating the margins of early gastric cancer in magnifying narrow-band imaging endoscopy. Endoscopy. 2021;53(5):469–77.
23. Li J, Zhu Y, Dong Z, et al. Development and validation of a feature extraction-based logical anthropomorphic diagnostic system for early gastric cancer: a case-control study. EClinicalMedicine. 2022;46: 101366.
24. Dong Z, Wang J, Li Y, et al. Explainable artificial intelligence incorporated with domain knowledge diagnosing early gastric neoplasms under white light endoscopy. NPJ Digit Med. 2023;6(1):64.
25. Du H, Dong Z, Wu L, et al. A deep-learning based system using multimodal data for diagnosing gastric neoplasms in real-time (with video). Gastric Cancer. 2023;26(2):275–85.
26. Ma T, Liu GQ, Guo J, et al. Artificial intelligence-aided optical biopsy improves the diagnosis of esophageal squamous neoplasm. World J Gastroenterol. 2025;31(13): 104370.
27. Guleria S, Shah TU, Pulido JV, et al. Deep learning systems detect dysplasia with human-like accuracy using histopathology and probe-based confocal laser endomicroscopy. Sci Rep. 2021;11(1):5086.
28. Taunk P, Atkinson CD, Lichtenstein D, Rodriguez-Diaz E, Singh SK. Computer-assisted assessment of colonic polyp histopathology using probe-based confocal laser endomicroscopy. Int J Colorectal Dis. 2019;34(12):2043–51.
29. Cho H, Moon D, Heo SM, et al. Artificial intelligence-based real-time histopathology of gastric cancer using confocal laser endomicroscopy. NPJ Precis Oncol. 2024;8(1): 131.
30. Szegedy C, Ioffe S, Vanhoucke V, Alemi A. AAAI; 2016;31 Available from: https://arxiv.org/abs/1602.07261
31. Du Y, Bai Y, Xie P, et al. Chronic gastritis in China: a national multi-center survey. BMC Gastroenterol. 2014;14:21.
32. Dixon MF. Gastrointestinal epithelial neoplasia: Vienna revisited. Gut. 2002;51(1):130–1.
33. Hunter JD. Matplotlib: A 2D graphics environment. Comput Sci Eng. 2007;9:90–5.
34. Park JC, Park Y, Kim HK, et al. Probe-based confocal laser endomicroscopy in the margin delineation of early gastric cancer for endoscopic submucosal dissection. J Gastroenterol Hepatol. 2017;32(5):1046-54. https://doi.org/10.1111/jgh.13635.
35. Pimentel-Nunes P, Libânio D, Marcos-Pinto R, et al. Management of epithelial precancerous conditions and lesions in the stomach (maps II): European Society of gastrointestinal endoscopy (ESGE), European Helicobacter and microbiota Study Group (EHMSG), European Society of pathology (ESP), and Sociedade Portuguesa de Endoscopia Digestiva (SPED) guideline update 2019. Endoscopy. 2019;51(4):365–88.
36. Pittayanon R, Rerknimitr R, Wisedopas N, et al. Flexible spectral imaging color enhancement plus probe-based confocal laser endomicroscopy for gastric intestinal metaplasia detection. J Gastroenterol Hepatol. 2013;28(6):1004–9.

Publisher's Note

Springer Nature remains neutral with regard to jurisdictional claims in published maps and institutional affiliations.